Hindawi Publishing Corporation
Mathematical Problems in Engineering
Volume 2014, Article ID 919681, 10 pages
http://dx.doi.org/10.1155/2014/919681

Research Article

Pulse Sign Separation Technique for the Received Bits in Wireless Ultra-Wideband Combination Approach

Rashid A. Fayadh,[1] F. Malek,[2] and Hilal A. Fadhil[1]

[1] *School of Computer and Communication Engineering, Universiti Malaysia Perlis (UniMAP), 02000 Arau, Perlis, Malaysia*
[2] *School of Electrical Systems Engineering, Universiti Malaysia Perlis (UniMAP), 02600 Arau, Perlis, Malaysia*

Correspondence should be addressed to Rashid A. Fayadh; r_rashid47@yahoo.com

Received 10 November 2013; Accepted 16 June 2014; Published 6 July 2014

Academic Editor: Chunlin Chen

When receiving high data rate in ultra-wideband (UWB) technology, many users have experienced multiple-user interference and intersymbol interference in the multipath reception technique. Structures have been proposed for implementing rake receivers to enhance their capabilities by reducing the bit error probability (P_e), thereby providing better performances by indoor and outdoor multipath receivers. As a result, several rake structures have been proposed in the past to reduce the number of resolvable paths that must be estimated and combined. To achieve this aim, we suggest two maximal ratio combiners based on the pulse sign separation technique, such as the pulse sign separation selective combiner (PSS-SC) and the pulse sign separation partial combiner (PSS-PC) to reduce complexity with fewer fingers and to improve the system performance. In the combiners, a comparator was added to compare the positive quantity of positive pulses and negative quantities of negative pulses to decide whether the transmitted bit was 1 or 0. The P_e was driven by simulation for multipath environments for impulse radio time-hopping binary phase shift keying (TH-BPSK) modulation, and the results were compared with those of conventional selective combiners (C-SCs) and conventional partial combiners (C-PCs).

1. Introduction

The explosive growth of indoor wireless devices that has occurred in the market is expected to continue for the foreseeable future. The modern generation of wireless systems aims to provide flexible medium or high data rates and a wide variety of applications, such as ranging and video to serve several users. The goal of this research is to reduce the probability of bit errors at the receiving part of wireless systems and to face the growing spectral requirements of other narrow-band systems. Ultra-wideband transmission power of −41.3 dBm/MHz and the frequency range of 3.1 to 10.6 GHz were established by the Federal Communications Commission (FCC) in the United States [1]. UWB is an impulse radio (IR) that is based on short-time transmitted pulses, in the order of nanoseconds, and low level power pulses, which interfere as a noise power level because the signals' power is spread over the UWB bandwidth in established and licensed spectral regions [2]. Direct sequence (DS) spreading and time-hopping spreading implementations are used to employ different types of digital modulations, such as pulse amplitude modulation (PAM), on-off keying (OOK), pulse position modulation (PPM), and phase shift keying (PSK) [3]. In UWB applications, the binary phase shift keying (BPSK) modulation technique is popular due to its smooth power spectrum and low bit error rate (BER) [4]. The BPSK modulation was used in this work with a sequence of pulses that were transmitted over a large number of frames in time-hopping spread spectrum technology in the presence of intersymbol interference (ISI) and multiple-user interference (MUI). In addition, the UWB systems receive interference from narrow-band systems and the mitigation of this problem is not considered in the current work because it has been addressed in other papers [5, 6].

A stream of multipath components (MPCs) can be resolved to allow rake receivers to extract the individual, multipath signals, and a new improved technique was developed by [7] for signal-stream and multiple-stream pre/postrake structures to maximize the received signal-to-noise ratio (SNR). MUI and ISI degrade the performance of multiuser detectors when communicating over UWB channels, and Hung and Chen [8] proposed Hopfield neural networks to reduce the computational complexity and to mitigate interference. Simulations in [9] were conducted using line-of-sight (LOS) paths and non-line-of-sight (NLOS) paths for adaptive selective-rake and adaptive partial-rake receivers, and the performance of these two receiver structures was investigated. Increasing the average received SNR was achieved by [10] by combining the selected strongest paths from several clusters with the first paths arriving in a limited duration out of the resolved MPCs. In the presence of MUI, selective-rake receivers have been developed to improve the performance of indoor wireless reception based on the mitigation of MUI additive white Gaussian noise (AWGN) disturbances [11] and based on adding interference-sensing (IS) devices [12].

Unfortunately, the optimal design of wireless receivers must overcome two problems to avoid MUI. First, the exact probability density function (pdf) of several users' interferences cannot lead to effective wireless receiver designs. Second, the existence of Gaussian white noise in the UWB system leads to full noise-pulse interference which complicates the convolution of the exact pdf of the MUI with that of the Gaussian noise [13]. These challenges encouraged us to propose a new technique in the combiner to decrease the effect of Gaussian noise on the desired pulse and to mitigate the MUI when receiving the pulses of many users. This paper presents the results of the simulation of the performance of the conventional and proposed selective-rake and partial-rake combiners in an indoor channel model (CM2) for UWB wireless propagation at NLOS paths. The work provided a direct relationship between the number of users and the number of resolved multipath components (MPCs) that used the MRC combiner, which is based on the pulse sign separation technique. This relationship indicated the probability of the number of positive pulses over negative pulses for receiving bit 1 and the probability of the number of negative pulses over positive pulses for receiving bit 0.

The remainder of this research is ordered as follows. Section 2 gives a brief overview of the time-hopped UWB system and the UWB channel model. Section 3 considers the multipath wireless receiver and the proposed MPCs combiner. Section 4 gives the simulation results and discussion of these results with the conventional combiner. Our conclusions are presented in Section 5.

2. TH-UWB System Scheme and Signal Model

In TH-UWB systems, the pulses are very narrow, that is, less than one nanosecond of pulse time (T_p) in each chip slot of length T_c, and, typically, each amount of chip slots is structured to frame the duration of the length of T_f, as shown in Figure 1; moreover, the number of chip slots depends on the number of users in the simulation. The transmitted data bits are frequently transmitted over several frames (N_f), and

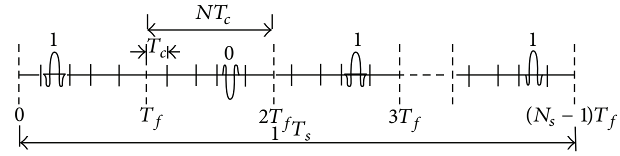

Figure 1: Frame structure of TH-BPSK UWB signals.

each frame contains a pulse that can be shifted to a different chip slot according to pseudo-random time-hopping code (C_i^u), where u is the defined user, (i) is the slot frame, and $C_i^u \in \{0, 1, \ldots, N_c - 1\}$ is considered to be larger than T_p to avoid collisions in the multipath access channels; $C_i^u \in \{0, 1, \ldots, N_c - 1\}$ is chosen to satisfy $T_c \le T_f / N_c$ to prevent interpulse interference (IPI). One information symbol of duration $T_s = N_f T_f$ is represented by a number of pulses (N_f) and denoted as $b_j^u \in \{+1, -1\}$ where it is transmitted by user u in the jth symbol. The basic signaling transmitted pulse $P_T(t)$ of duration T_p was analyzed to have a unit energy; that is, $\int_{-\infty}^{\infty} P_T^2(t) = 1$. The generation of a suitable signal is connected to the radio communication link, which is modulated with desired bits before transmission through wireless channels. Since the Gaussian waveforms are more popular for UWB transmissions, a Gaussian pulse $[g_0(t)]$ of zero mean and σ standard deviation was considered in the generating waveform, which is given by [14, 15] as follows:

$$g_0(t) = e^{-t^2/2\sigma^2}, \tag{1}$$

where $\sigma = \tau / 2\sqrt{\pi}$, and τ is the time shape factor, which was assumed to be 0.5 ns in this research. In this work, we considered second order derivatives $[g_2(t)]$ of a Gaussian function $e^{-2\pi(t/\tau)^2}$ as shown in Figure 2 to denote the $P_T(t)$ shaping form:

$$P_T(t) = \left[1 - 4\pi\left(\frac{t}{\tau}\right)^2\right] e^{-2\pi(t/\tau)^2}. \tag{2}$$

The transmitted signal $S_T^u(t)$ for the uth user and energy per bit using BPSK modulation can be written as

$$S_T^u(t) = \sqrt{\frac{E_b}{N_f}} \sum_{i=-\infty}^{\infty} C_{\lfloor i/N_f \rfloor}^u P_T\left(t - iT_f - C_i^u T_c\right), \tag{3}$$

where $\lfloor i/N_f \rfloor$ is the nearest integer less than

$$C_{\lfloor i/N_f \rfloor}^u = \sum_{j=0}^{N_f - 1} b_j^u w_i^u, \tag{4}$$

where w_i^u are the values of $\{\pm 1\}$ as binary random variables of the time-hopped BPSK signal, which can be written for the uth user as

$$S_T^u(t) = \sqrt{\frac{E_b}{N_f}} \sum_{i=-\infty}^{\infty} \sum_{j=0}^{N_f - 1} b_j^u w_i^u P_T\left(t - jT_s - iT_f - C_i^u T_c\right). \tag{5}$$

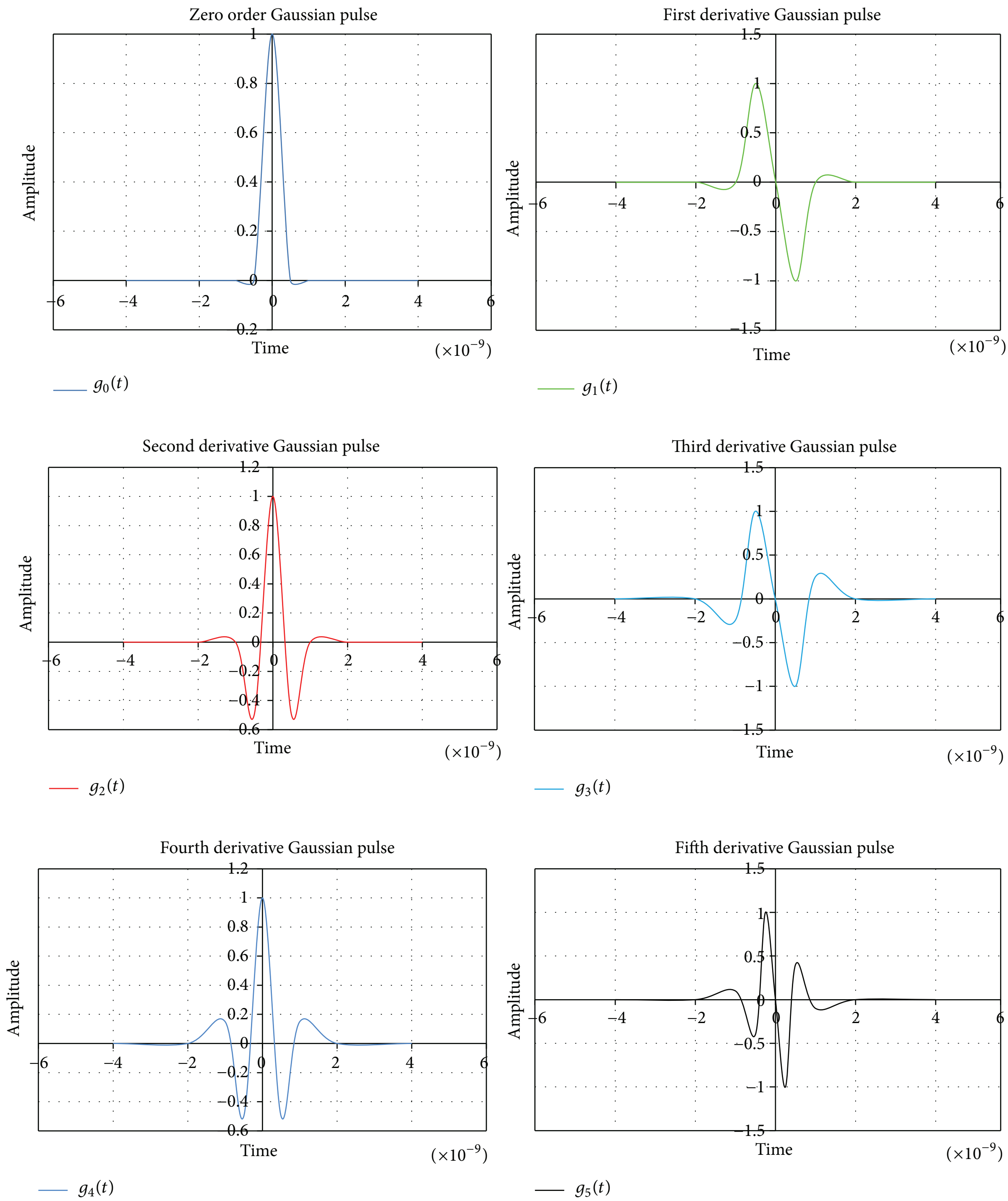

Figure 2: Five order derivatives of Gaussian pulse in time-domain representation [22].

Normally, wireless reception depends on multipath propagation between the transmitter and the receiver through indoor, outdoor, and farm environments. Four standard channel models, CM1, CM2, CM3, and CM4 were adopted by the IEEE 802.15.3a committee with parameters to cover line-of-sight (LOS) and non-line-of-sight (NLOS) transmission and reception paths [1]. In this work, we concentrated on the CM2 channel model of NLOS propagation, and a range of four meters was used in the simulation and analysis of UWB signal processing. Depending on obstacles fading, the spread copies of received pulse with different amplitudes due to multipath effects are illustrated in Figure 3, which requires suggesting a receiver of several demodulators and combiners to capture most of the pulse energy as shown in Figure 4. The UWB channel model rays (l) are clustered to k clusters, and each cluster contains a number of paths based on the

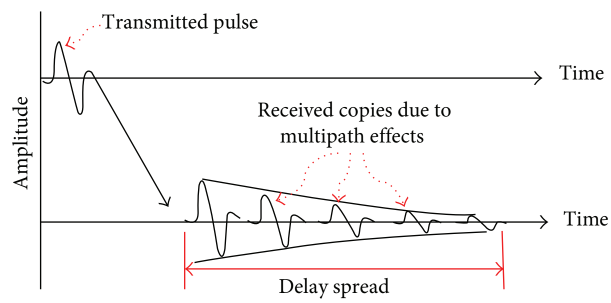

Figure 3: Received multipath pulse copies.

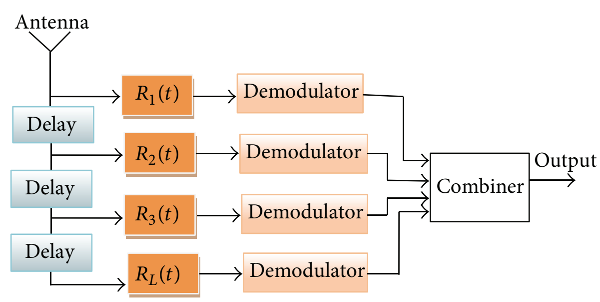

Figure 4: Several demodulators to receive the resolved and delayed multipath components.

number of rake fingers (demodulators or correlators) [16, 17]. The reception was considered to be over UWB channel frequency through indoor multipath propagation, and the channel discrete time impulse response $[h^u(t)]$ for user u can be modeled as

$$h^u(t) = X\sum_{l=0}^{L}\sum_{k=0}^{K} A^u_{k,l}\delta\left(t - T^u_k - \tau^u_{k,l}\right), \tag{6}$$

where X is the lognormal shadowing factor, $A^u_{k,l}$ are the channel multipath gain coefficients of the lth path within the kth cluster for user u, $\delta(\cdot)$ is the Dirac delta function, and $\tau^u_{k,l}$ is the delay of the lth multipath component relative to the kth cluster's arrival time T^u_k. To simplify the analysis, we assumed that the path resolution time was equal to the pulse duration (T_p) for the proposed wireless system. The arrival times of the rays and clusters were modeled by Poisson distribution, and their rates were denoted by Λ and λ, respectively. The multipath gain coefficient can be divided into three parts; that is,

$$A^u_{k,l} = p_{k,l}\xi_k\beta_{k,l}, \tag{7}$$

where $P_{k,l}$ is a random variable that has equal probability of taking the values of $+1$ or -1, ξ_l is a variable that represents the fading associated with the lth cluster, $\beta_{k,l}$ is the lognormal channel coefficient of the multipath ray l that belongs to the kth cluster, ξ_l reflects the fading associated with the kth cluster, and $\beta_{k,l}$ corresponds to the fading associated with the lth ray of the kth cluster. The $\xi_k\beta_{k,l}$ is distributed lognormally and jointly characterized by

$$20\log 10\left(\xi_k\beta_{k,l}\right) \propto \text{Normal}\left(\mu_{k,l}, \sigma_1^2 + \sigma_2^2\right)$$

$$\mu_{k,l} = \frac{10\ln\left(\Omega_0\right) - 10T_p/\Gamma - 10\tau_{k,l}/\gamma}{\ln(10)} - \frac{\left(\sigma_1^2 + \sigma_2^2\right)\ln(10)}{20}, \tag{8}$$

where Γ and γ are denoted as the cluster and ray decay factor, respectively, σ_1 is the standard deviation of the cluster lognormal fading term, σ_2 is the standard deviation of the ray lognormal fading term, and Ω_0 is the average power of the multipath component. The expectation $[E(\cdot)]$ of power profile decays for clusters and rays is expressed by exponential amplitude attenuations, and the lognormal shadowing variable term (X) is characterized as

$$\begin{gathered} E\left[\left|\xi_k\beta_{k,l}\right|^2\right] = \Omega_0 e^{-T_k/\Gamma} e^{-\tau_{k,l}/\gamma} \\ 20\log 10(X) \propto \text{Normal}\left(0, \sigma_x^2\right), \end{gathered} \tag{9}$$

where σ_x is the standard deviation of the lognormal shadowing term for the entire multipath process (dB). After transmission, the modulated signal over the CM2 channel model of $h^u(t)$ impulse response and the received signal $r^u_l(t)$ is the convolution process $(*)$ of the transmitted signal with

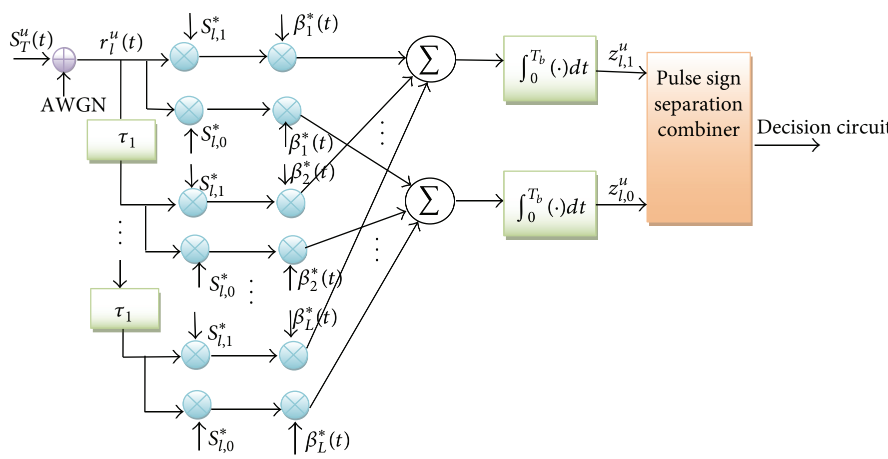

FIGURE 5: Optimum demodulators for UWB binary signals.

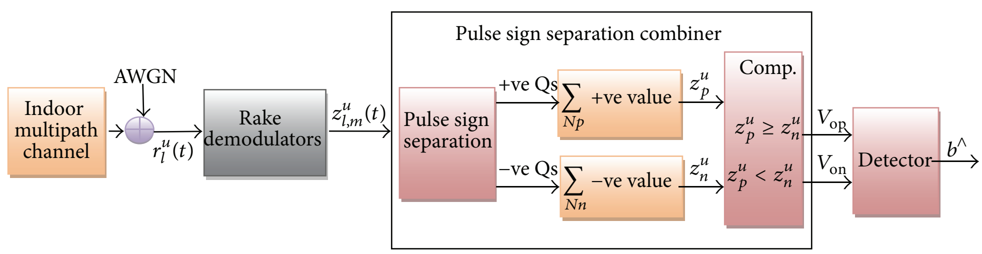

FIGURE 6: Block diagram of wireless receiver with the proposed pulse sign separation combiner.

the channel impulse response by adding a zero mean white Gaussian noise $n(t)$ [18]. Consider

$$r_l^u(t) = S_T^u(t) * h^u(t) + n(t)$$
$$r_l^u(t) = X\sqrt{\frac{E_b}{N_f}} \sum_{i=-\infty}^{\infty} \sum_{j=0}^{N_f-1} \sum_{l=0}^{L} \sum_{k=0}^{K} A_{k,l}^u b_j^u w_i^u P_T \times \left(t - jT_s - iT_f - c_i^u T_c - T_k^u - \tau_{k,l}^u\right) + n(t). \tag{10}$$

For optimum demodulator, we considered binary signaling over the previous channel model of time-variant weights $\{\beta_l^*(t)\}$, where $l = 1, 2, \ldots, L$, and two equal-energy signals $s_{l,0}^*$ and $s_{l,1}^*$ which are the same transmitted signals and are selected by delay duration to satisfy the multipath components duration. We supposed that the channel tap weights were known, cross correlation employment in the demodulator, and perfect synchronization. The template UWB signals are generated from pseudo-random sequences which have the property of cross correlation resulting signals over the bit duration (T_b). Consider

$$\int_0^{T_b} s_{l,m}(t-\tau_l)\, s_{l,m}^*(t-\tau_l)\, dt, \quad m = 0, 1. \tag{11}$$

The signal of bit 0 at each tap correlates with $\beta_l^*(t)\ s_{l,0}^*(t)$ and the signal of bit 1 correlates with $\beta_l^*(t)\ s_{l,1}^*(t)$ as shown in the receiver structure of Figure 5. The output of correlators $z_{l,1}^u(t)$ and $z_{l,0}^u(t)$ with delayed by τ_l template signal $\{s_{l,m}^*(t-\tau_l)$, where $m = 0, 1\}$ and $(\cdot)^*$ denotes complex conjugation, which can be expressed as

$$\begin{aligned}
z_{l,1}^u &= \mathrm{Re}\left[\sum_{l=1}^{L} \int_0^{T_b} r_l^u(t)\, \beta_l^*(t)\, s_{l,1}(t-\tau_l)\, s_{l,1}^*(t-\tau_l)\, dt\right] \\
&\quad + \mathrm{Re}\left[\sum_{l=1}^{L} \int_0^{T_b} n(t)\, \beta_l^*(t)\, s_{l,1}^*(t-\tau_l)\, dt\right] \\
z_{l,0}^u &= \mathrm{Re}\left[\sum_{l=1}^{L} \int_0^{T_b} r_l^u(t)\, \beta_l^*(t)\, s_{l,0}(t-\tau_l)\, s_{l,0}^*(t-\tau_l)\, dt\right] \\
&\quad + \mathrm{Re}\left[\sum_{l=1}^{L} \int_0^{T_b} n(t)\, \beta_l^*(t)\, s_{l,0}^*(t-\tau_l)\, dt\right].
\end{aligned} \tag{12}$$

3. The Proposed Combiner

The received signals are a large number of arriving multipath components (MPCs) with varying time delays. Therefore, large losses occur in the energy of the received signal which leads to the use of a rake-demodulator type receiver to receive a number of resolved MPCs reducing the fading effects [19]. As the transmitted information is modulated by BPSK modulation, a single matched filter is required to demodulate

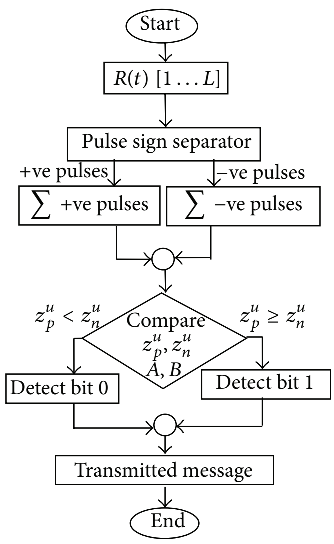

FIGURE 7: Simulation flow chart of the research project.

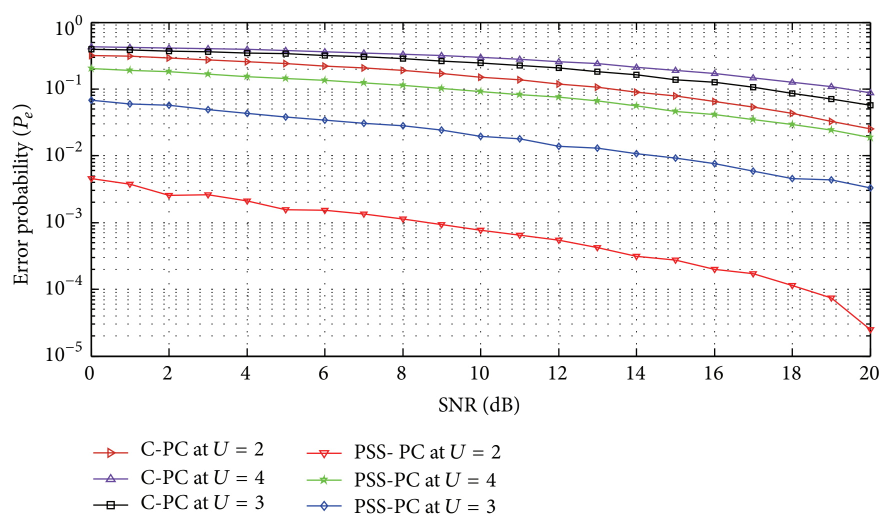

FIGURE 8: Error probability performance versus SNR of partial combiner for $L_p = 10$ paths in CM2.

the transmitted signal $S_T^u(t)$ from the Lth channel. The signal $S_T^u(t)$ is positive at transmitted bit 1 and negative at transmitted bit 0 and is equal in amplitude. A combiner follows the demodulators to achieve the best performance for the wireless receiver, assuming perfect estimation of the channel. The maximal ratio combiner (MRC) technique was used to combine different attenuation, shifted, and delayed signals received after selecting the L paths by best paths selection (selective combining) or by partial selection (partial combining) [20]. In selective combining, L best paths are selected from all resolved MPCs so that it is necessary to keep track of all path components. In partial combining, the first L arrived paths are selected for combining components with lower performance and less complexity than the selective combiner [21].

The received signal passes through the linear filter of the demodulator and is matched with the received pulse, as shown in Figure 6, and is then sampled at the chip rate of 100 GHz. Each branch of the rake demodulator has a delay time related to the first branch, and the output signal ($Y_{l,m}^u$) to the combiner is encumbered by intersymbol interference (ISI), multiuser interference (MUI), and adaptive white Gaussian noise (AWGN). The combiner input signal is in a vector form for the sth symbol of the uth user. The lth branch can be formulated in matrix form, user one is assumed to be the desired user, and her or his delay is 0 at the receiver. This signal contains the noise and interference which can be formulated as

$$Y_{l,m}^u(t) = z_{l,m}^u(t) + \text{ISI} + \text{MUI} + \text{AWGN}, \qquad (13)$$

where $Y_{l,m}^u(s)$ is the input sampled signal to the pulse sign separation combiner with the noise mixing of white Gaussian,

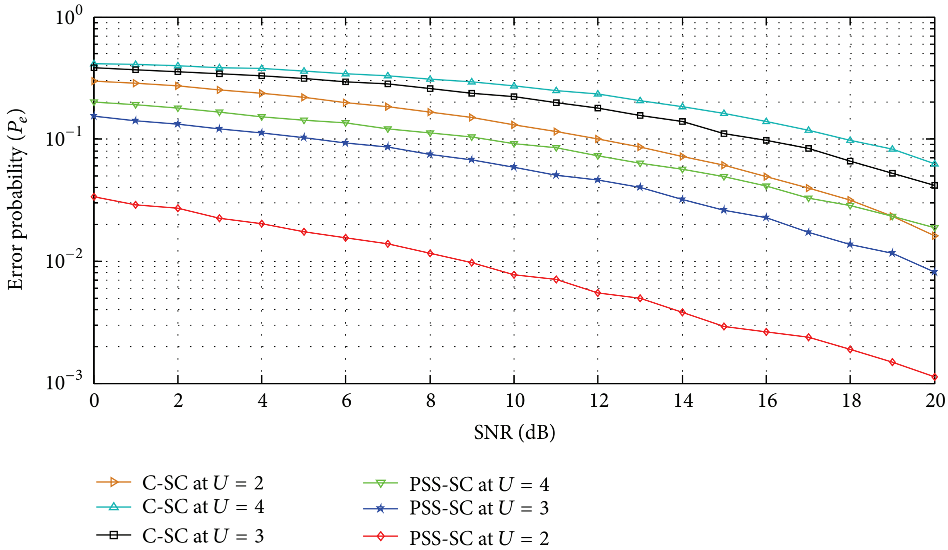

FIGURE 9: Error probability performance versus SNR of selective combiner for $L_s = 10$ paths in CM2.

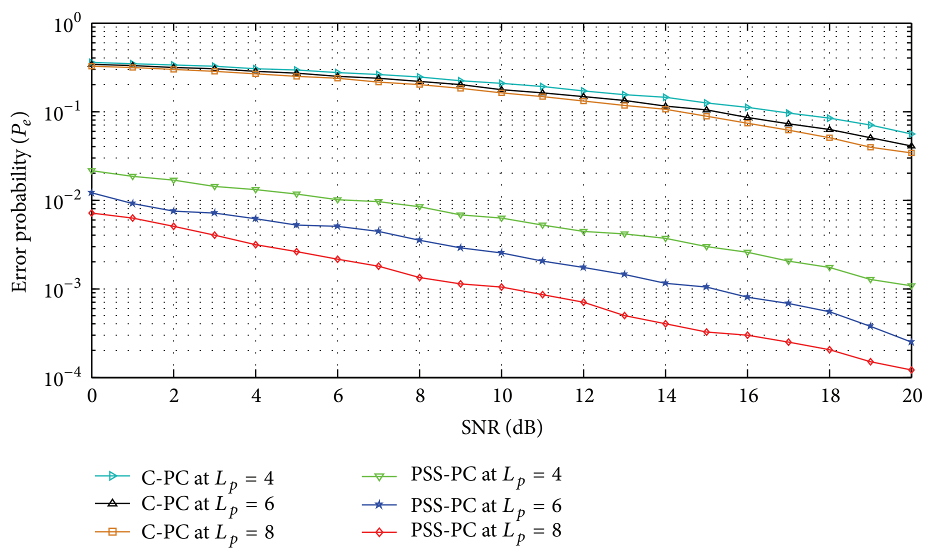

FIGURE 10: Error probability performance versus SNR of partial combiner with two users in CM2.

intersymbol interference, and multiuser interference when using the proposed research for many users. Consider

$$Y_{l,m}^{u}(t) = X_l D + X_l I_1 + X_l I_2 + n_l(t), \tag{14}$$

where D is the desired signal, I_1 is the MUI term, X is fading coefficients for lth paths, and I_2 is the ISI term. Because the demodulator output pulses are corrupted by interferences and fading, to overcome fading and improve reception, these pulses are separated by pulse sign separation device to get a number of positive pulses (+ve Qs) and a number of negative pulses (−ve Qs) separately. These pulses are combined to create the overall positive signal (z_p^u) or overall negative signal (z_n^u) through the combiner gain or weighting coefficients (α_l), which are multiplied by the outputs of the demodulators. Consider

$$\begin{aligned} z_n^u &= \sum_{l=+ev}^{P} \alpha_l Y_{l,m}^{u}(t) \quad l = 1,\ldots,P,\ m = 0,1 \\ z_p^u &= \sum_{l=-ev}^{N} \alpha_l Y_{l,m}^{u}(t) \quad l = 1,\ldots,N,\ m = 0,1 \\ \alpha_l &= \frac{\left[Y_{l,m}^{u}(t)\right]^2}{\sum_{l=1}^{L}\left[Y_{l,m}^{u}(t)\right]^2}. \end{aligned} \tag{15}$$

The performance of the supposed wireless receiver is to determine the bit-error probability (P_e) compared with the values of signal-to-noise ratio (SNR). The corresponding P_e

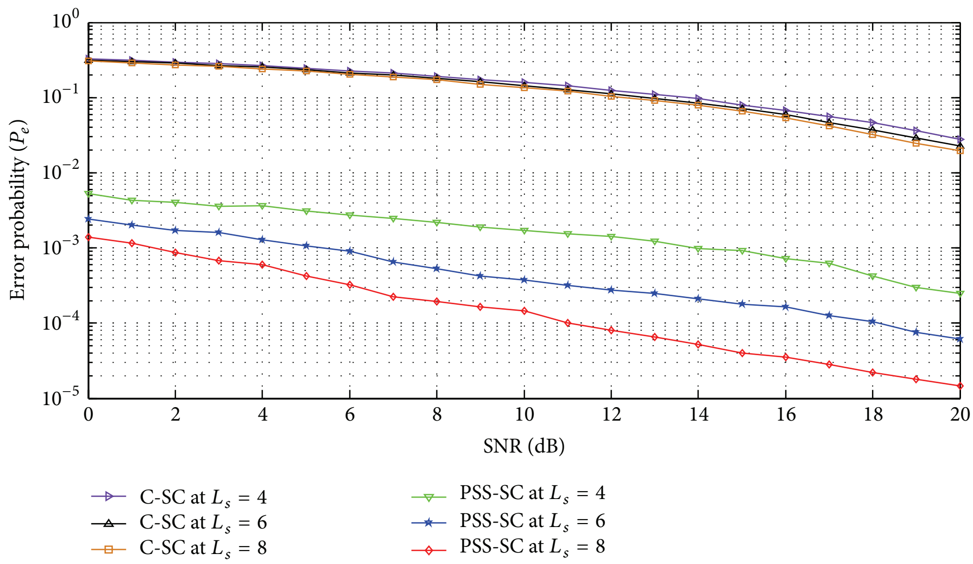

Figure 11: Error probability performance versus SNR of selective combiner with two users in CM2.

Table 1: Comparison of signals.

Comparator output	V_{op}	V_{on}
$z_p^u \geq z_n^u$	1	0
$z_p^u < z_n^u$	0	1

for BPSK in one particular channel realization for antipodal signals can be defined in the modeled form as

$$P_e(\gamma_b) = Q\left(\sqrt{2\gamma_b}\right)$$
$$\gamma_b = \sum_{l=1}^{l} \gamma_l$$
$$\gamma_l = \frac{E_b(l)}{N_0}$$
$$E_b(l) = \sum_{l=1}^{L} \alpha_l^2, \qquad (16)$$

where $Q(\cdot)$ stands for Q function, $E_b(l)$ is the bit energy at lth path, and γ_l and γ_b are the received energy per bit, the SNR for lth UWB channel realization, and the SNR for one bit, respectively. In the selective combiner, the mean-square values of α_l are selected as the strongest multipath components from a vector of their positions in one channel realization. However in the partial combiner, the mean-square values of α_l are selected for first arrival multipath components.

The summation results, z_p^u and z_n^u, are sent to the comparator to compare them. The output amplitudes (V_{op} and V_{on}) of the comparator, as presented in Table 1, are passed to the decision circuit which selects the largest output of the corresponding signal in order to decide whether the detected bit ($b^\wedge$) is 1 or 0, which is based on the following criteria:

$$b^\wedge = \begin{cases} 1 & \text{if } z_p^u \geq z_n^u \\ 0 & \text{if } z_p^u < z_n^u. \end{cases} \qquad (17)$$

4. Simulation Results and Discussion

By using MATLAB simulation software, the CM2 multipath channel model was run with seven key model measurement parameters, that is, Λ (1/nsec) of 0.4, λ (1/nsec) of 0.5, Γ (nsec) of 5.5, γ (nsec) of 6.7, σ_1 (dB) of 3.3941, σ_2 (dB) of 3.3941, and σ_x (dB) of 3 [1]. Figure 7 shows the flow chart of the proposed combiner simulation, and the previous parameters in the calculation of specific simulation were maintained similarly for the conventional and proposed combiners in order to obtain an impartial comparison.

The analysis and simulated results were based on the indoor non-line-of-sight (NLOS) multipath channel model (CM2) with a range of four meters. Selective combining (SC) and partial combining (PC) combiners were simulated using MATLAB software to determine the advantage of capturing the strongest paths signals and the first arriving paths, respectively. The transmitted bits were generated randomly and assumed to be 40,000 bits. The shaping factor for the pulse was 0.22 ns with N_s = 5 pulses per bit and the transmitted bits were modulated using BPSK modulation. Several simulations were performed to represent the probability of error after averaging the values over 50 channels, and the SNR was varied from 0 to 20 dB to confirm the performance of the proposed combiners. The performance evaluation of the proposed pulse sign separation partial combining (PSS-PC) combiner is illustrated in Figure 8 for two, three, and four users through 10 NLOS paths and the conventional partial combiner (C-PC) in the CM2 multipath channel model. In addition, under CM2 channel parameters, the

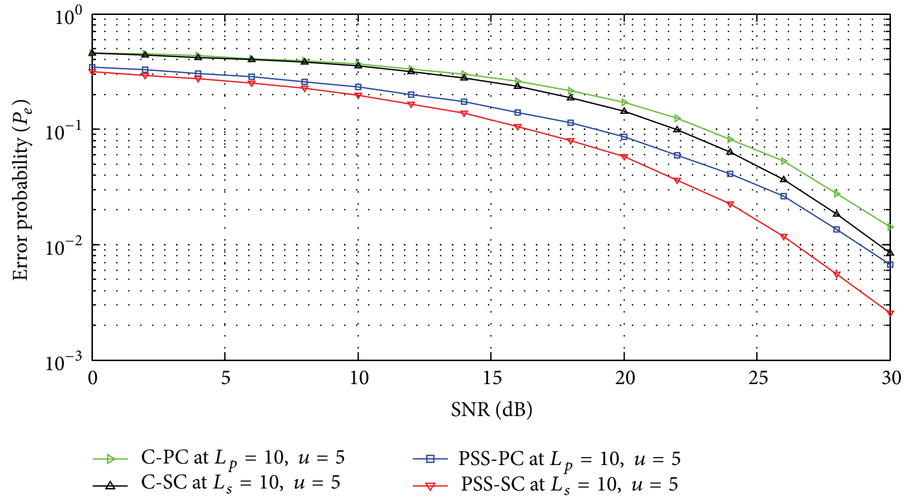

Figure 12: Error probability of bit rate versus SNR of the suggested combiner within ten paths and five users in CM2.

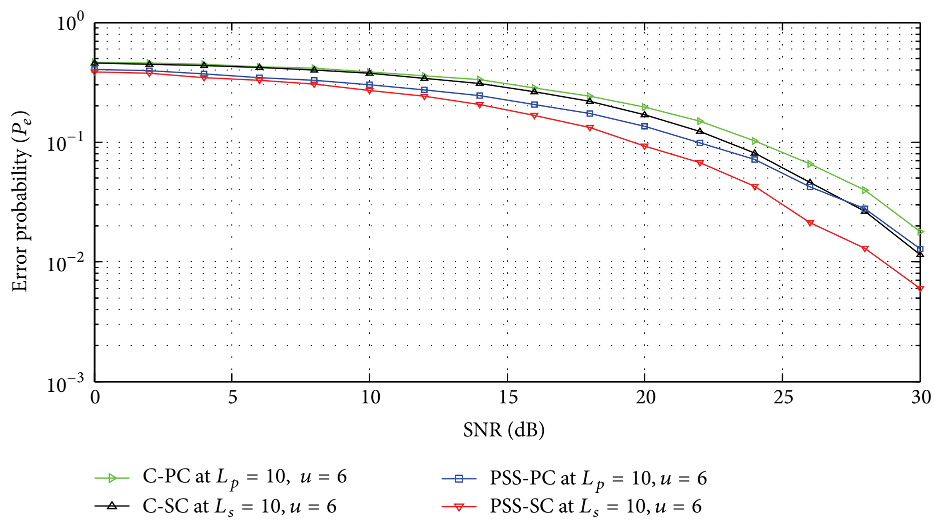

Figure 13: Error probability of bit rate versus SNR of the suggested combiner within ten paths and six users in CM2.

characteristics of the proposed pulse sign separation selective combining (PSS-SC) combiner are shown in Figure 9 with interesting results for error probability when compared with the conventional selective combiner (C-SC) for two, three, and four users through 10 NLOS paths. Figure 10 shows the BER versus SNR for PSS-PC in the same channel model; the probability of error decreased as the number of paths increased from four to eight with a concentration of two users, and the same behavior is shown in Figure 11 for the PSS-SC combiner compared with C-PC and C-SC, respectively. The comparison results are provided in Table 2 between the proposed and conventional combiners depending on error probability values when the powers of signal and noise are equal to give a signal-to-noise ratio (SNR) of 0 dB.

The simulation software was run again for both conventional and proposed combiners to show the performance of the suggested combiners for five and six users when $L_p = 10$ and $L_s = 10$ in CM2 channel conditions. Twenty thousand bits and five or six pulses per frame were generated using TH-BPSK modulation. The pulse duration was taken to be 0.22 ns, less than the chip duration of 0.5 ns, to reduce the interference due to user pulses. In comparison with the conventional combiner, Figure 12 shows the bit rate error probability versus SNR for PSS-PC and PSS-SC combiners in the same channel model. The probability of error decreased from 0.45 to 0.35 and from 0.45 to 0.31, respectively, for five users at an SNR of 0 dB. The simulation run was repeated with CM2 channel parameters for partial and selective combiners at 10 diversity paths and six users. Figure 13 shows the simulation results for the proposed partial and selective combiners with conventional ones. From these figures, it can be concluded that the PSS-PC and PSS-SC combiners have an advantage of reducing the probability of error with a higher number of diverse paths or lower number of users, thereby leading to improved performance.

Table 2: Error probability performances with varying numbers of paths and users.

Combiner	No. of users (U)	P_e at 10 paths	No. of paths	P_e at 2 users
C-PC	4	0.42	$L_p = 4$	0.38
	3	0.39	$L_p = 6$	0.35
	2	0.30	$L_p = 8$	0.32
PSS-PC	4	0.21	$L_s = 4$	0.022
	3	0.16	$L_s = 6$	0.014
	2	0.033	$L_s = 8$	0.0071
C-SC	4	0.43	$L_p = 4$	0.32
	3	0.40	$L_p = 6$	0.30
	2	0.31	$L_p = 8$	0.28
PSS-SC	4	0.20	$L_s = 4$	0.0052
	3	0.16	$L_s = 6$	0.0025
	2	0.032	$L_s = 8$	0.0015

5. Conclusions

In this paper, depending on the likelihood of a smaller number of erroneous pulses being received, the pulse sign separation combiner was used to separate the sign of pulses and combine the outputs of the rake demodulators for the TH-UWB system presented. The two proposed combiners for UWB applications, PSS-PC and PSS-SC combiners, were simulated and analyzed using MATLAB software to show system performance by reducing bit error rate probability. The suggested selective and partial combiners were compared with the conventional selective and partial combiners, which led to the improvement of performances without increasing the complexity of the receiver under CM2 channel model conditions.

Conflict of Interests

The authors declare that there is no conflict of interests regarding the publication of this paper.

References

[1] A. F. Molisch, J. R. Foerster, and M. Pendergrass, "Channel models for ultrawideband personal area networks," *IEEE Wireless Communications*, vol. 10, no. 6, pp. 14–21, 2003.

[2] H. Nikoogar and R. Prasad, *Introduction to Ultra Wideband for Wireless Communications*, Springer, Berlin, Germany, 2009.

[3] J. G. Prokis, *Digital Communications*, McGraw-Hill International Press, 4th edition, 2001.

[4] D. Tse and P. Viswanath, *Fundamentals of Wireless Communication*, Cambridge University Press, 2005.

[5] B. Hu and N. C. Beaulieu, "Performance of an ultra-wideband communication system in the presence of narrowband BPSK- and QPSK-Modulated OFDM interference," *IEEE Transactions on Communications*, vol. 54, no. 10, pp. 1720–1724, 2006.

[6] N. Boubaker and K. B. Letaief, "MMSE multipath diversity combining for multi-access TH-UWB in the presence of NBI," *IEEE Transactions on Wireless Communications*, vol. 5, no. 4, pp. 712–719, 2006.

[7] X. Cheng and Y. L. Guan, "Pre/post-rake diversity combining for UWB communications in the presence of pulse overlap," *IEEE Transactions on Wireless Communications*, vol. 11, no. 2, pp. 481–487, 2012.

[8] H.-L. Hung and H.-C. Chen, "Multi-user detection in ultra-wideband multiple-access communications systems using an efficient heuristic algorithm," *Scientific Research and Essays*, vol. 7, no. 9, pp. 1058–1069, 2012.

[9] A. P. Doukeli, A. S. Lioumpas, G. K. Karagiannidis, and P. V. Frangos, "Increasing the efficiency of rake receivers for ultra-wideband applications," *Wireless Personal Communications*, vol. 62, no. 3, pp. 715–728, 2012.

[10] F. Crăciun, I. Marghescu, and O. Fratu, "RAKE receiver performances for PAM-TH-UWB systems," in *Proceedings of the 19th Telecommunications Forum (TELFOR '11)*, pp. 289–292, IEEE, Belgrade, Serbia, November 2011.

[11] N. C. Beaulieu and D. J. Young, "Designing time-hopping ultrawide bandwidth receivers for multiuser interference environments," *Proceedings of the IEEE*, vol. 97, no. 2, pp. 255–284, 2009.

[12] D. J. Young and N. C. Beaulieu, "Time-hopped ultrawide bandwidth receiver designs using multiuser interference sensing," in *Proceedings of the IEEE International Conference on Ultra-Wideband (ICUWB '11)*, pp. 34–38, September 2011.

[13] N. C. Beaulieu and B. Hu, "Soft-limiting receiver structures for time-hopping UWB in multiple-access interference," *IEEE Transactions on Vehicular Technology*, vol. 57, no. 2, pp. 810–818, 2008.

[14] M. Z. Win and R. A. Scholtz, "Ultra-wide bandwidth time-hopping spread-spectrum impulse radio for wireless multiple-access communications," *IEEE Transactions on Communications*, vol. 48, no. 4, pp. 679–689, 2000.

[15] G. Durisi and S. Benedetto, "Performance evaluation of TH-PPM UWB systems in the presence of multiuser interference," *IEEE Communications Letters*, vol. 7, no. 5, pp. 224–226, 2003.

[16] A. A. Saleh and R. A. Valenzuela, "A statistical model for indoor multipath propagation," *IEEE Journal on Selected Areas in Communications*, vol. 5, no. 2, pp. 128–137, 1987.

[17] A. Mohsenian-Rad, J. Mietzner, R. Schober, and V. W. S. Wong, "Pre-equalization for pre-rake DS-UWB systems with spectral mask constraints," *IEEE Transactions on Communications*, vol. 59, no. 3, pp. 780–791, 2011.

[18] A. P. Adsul and S. K. Bodhe, "Performance evaluation of IR-UWB transceiver system using PPV," *Journal of Information and Operations Management*, vol. 3, no. 1, pp. 228–231, 2012.

[19] V. Niemelä, M. Hämäläinen, J. Iinatti, and A. Taparugssanagorn, "P-rake receivers in different measured WBAN hospital channels," in *Proceedings of the 5th International Symposium on Medical Information and Communication Technology (ISMICT '11)*, University of Oulu, Oulu, Finland, 2011.

[20] T. Chang, C. Chi, and Y. Chang, "Space-time selective RAKE receiver with finger selection strategies for UWB overlay communications," *IEEE Transactions on Microwave Theory and Techniques*, vol. 54, no. 4, pp. 1731–1744, 2006.

[21] M. Thériault, L. A. Rusch, S. Roy, and P. Fortier, "A semi-analytic method for BER performance of Rake-based UWB receivers," in *Proceedings of the IEEE Wireless Communications and Networking Conference (WCNC '08)*, pp. 112–117, April 2008.

[22] S. Li, *Adaptive interference suppression algorithms for DS-UWB systems [Ph.D. thesis]*, University of York, October 2010.